Electrical Power and Energy Systems 78 (2016) 445–454

Contents lists available at ScienceDirect

Electrical Power and Energy Systems

journal homepage: www.elsevier.com/locate/ijepes

Optimal active and reactive nodal power requirements towards loss minimization under reverse power flow constraint defining DG type

Aggelos S. Bouhouras [a,b,*], Kallisthenis I. Sgouras [a], Paschalis A. Gkaidatzis [a], Dimitris P. Labridis [a]

[a] Department of Electrical and Computer Engineering, Aristotle University of Thessaloniki, 54124 Thessaloniki, Greece
[b] Department of Electrical Engineering, Technological Educational Institute of Western Macedonia, 50100 Kozani, Greece

ARTICLE INFO

Article history:
Received 27 February 2015
Received in revised form 1 December 2015
Accepted 9 December 2015

Keywords:
Distributed generation
Optimal siting and sizing
Optimal DG number
Reverse power flow

ABSTRACT

In this paper a novel approach regarding the optimal penetration of Distributed Generation (DG) in Distribution Networks (DNs) towards loss minimization is proposed. More specific, a Local Particle Swarm Optimization (PSO) variant algorithm is developed in order to define the optimal active and reactive power generation and/or consumption requirements for the optimal number and location of nodes that yield loss minimization. Thus, the proposed approach provides the optimal number, siting and sizing of DGs altogether. In addition, based on the optimal power requirements of the resulted nodes, a combination of potential DG types to be installed is recommended. The proposed objective function in this paper is also innovative since it embeds the constraint of reverse power flow to the slack bus by the formation of a new penalty term. The proposed methodology is applied to 30 and 33 bus systems. The results indicate the optimal number, locations, and capacity of DG units, which were calculated simultaneously. Finally, the impact of the predefined amount of permissible reverse power flow to the optimal solution is also examined through two scenarios: the first considers zero reverse power flow and the second unlimited reverse power flow.

Introduction

The idea of Distributed Generation (DG) has forced researchers and engineers to change traditional perspectives regarding both the operation and planning of Distribution Networks (DNs). Several socioeconomic and environmental issues have established the penetration of Renewable Energy Sources (RESs) in DNs, mainly under the form of dispersed power units. Therefore, a lot of attention has been given towards the optimal installation of such power units by terms of appropriate placement along with optimal capacity [1]. The core concept of these optimal siting and sizing approaches relies on facing operational issues of DNs like power loss minimization [2], reliability improvement [3], voltage profile improvement [4] and more, by the most efficient way. The installation of DG units, either as small conventional power units or RESs, is expected to contribute in power loss reduction due to decreased branch currents that will result from local power production close to load demand. Therefore, the problem of defining the optimal siting and sizing of the dispersed power units towards loss minimization is mainly approached by examining the optimal locations to host these units along with their optimal capacity.

The main disadvantage, though, of all these aforementioned efforts relies on the absence of a new aspect regarding the operation of DNs under high penetration levels of DGs and RESs, namely the reverse power flow. Distribution System Operators (DSOs) have realized [5–11] that the adopted policy regarding the DG and RESs penetration without proper planning in order to evaluate their impact in a long term basis, has caused some new problems. In many cases, it is observed that specific parts of the DNs undergo reverse power flow due to high penetration of DGs or high power production of DG especially during time periods with low load demand. This results in upstream power flow with increased branch currents and potentially increased power losses. Thus, appropriate consideration should be taken into account about the formulated objective function.

In this paper, the problem of defining the optimal DG type to be installed by terms of location and capacity, subject to reverse power flow constraints, is examined with a Particle Swarm Optimization Algorithm (PSO) under a new and more deregulated perspective. More specific, a novel algorithm is proposed to deal with loss minimization in DNs under the constraint of no reverse power flow through the slack bus of the network. Thus, regardless the direction of the power flow within the radial DN, the main feeder

* Corresponding author at: Department of Electrical and Computer Engineering, Aristotle University of Thessaloniki, 54124 Thessaloniki, Greece.

E-mail addresses: abouchou@auth.gr (A.S. Bouhouras), ksgouras@ee.auth.gr (K.I. Sgouras), pgkaidat@auth.gr (P.A. Gkaidatzis), labridis@auth.gr (D.P. Labridis).

http://dx.doi.org/10.1016/j.ijepes.2015.12.014
0142-0615/

in the slack bus should not experience upstream power flow. This approach means that it is allowed for any internal branch to undergo reverse power flow, given that this could contribute in further loss reduction in respect to the situation with only downstream power flow through the main feeder of the DN. Moreover, in this work the proposed algorithm provides the optimal active and reactive power generation and/or compensation for the optimal number of candidate nodes to host DG units and compensators. Thus, based on each node's power requirements, the type of DG units could be in turn easily defined. Hence, instead of investigating how specific types of DG units should be optimally installed in the DN [12–17], the number and types of DG units could be defined due to each node's power consumption and/or generation demands. Therefore the scope of this work relies on solving the conventional Optimal Distributed Generation Problem (ODGP) by including the additional constraint of the reverse power flow in the objective function. Although the analysis in this work considers both active and reactive power production by the DG units, it should be clarified that the consideration of the reverse power flow in the ODGP problem is not correlated with any kind of real time power control of the DG units.

This paper is organized as follows: in Section 'Proposed algorithm' the proposed algorithm with the novel objective function is presented. Section 'DN under study and penetration scenarios' includes the DN for the algorithm implementation along with the examined scenarios. Section 'Results' presents the results of the analysis and finally, in Section 'Conclusion' the derived conclusions are discussed.

Proposed algorithm

The contribution of this paper relies firstly on the development of a novel algorithm that provides for a given DN the optimal siting, sizing and number of DG units altogether. A part of the published literature [14,18–20] deals with the problem by facing only the siting and sizing of DG and in many cases this is performed under a sequential approach or by ranking locations [21] and not simultaneously. In these aforementioned cases though, the number of DG units to be installed is predefined, hence the solution could not be considered as an optimal by terms of optimum DG units number. The second contribution of this work refers to the consideration of the reverse power flow constraint in the objective function and its impact to the optimal solution. Finally, the third contribution of the algorithm involves a recommendation of the appropriate types of DG units to be installed based on the power demand and/or generation requirements for the indicated nodes by the algorithm. Each contribution is analyzed at the respective section of the paper, where it is presented.

Objective function

The penetration of DGs in DNs is expected to yield decreased branch currents and thus to contribute in loss reduction. Therefore, the objective/target function in this work is formulated [22] by terms of power loss minimization and is expressed as follows:

$$F_{loss} = \min \sum_{\substack{i,j=1 \\ i \neq j}}^{n_l} g_{i,j}\left(V_i^2 + V_j^2 - 2V_iV_j\cos(\theta_i - \theta_j)\right) \quad (1)$$

where

V_i is the voltage magnitude of bus i,
V_j is the voltage magnitude of bus j,
$g_{i,j}$ is the conductance between buses i and j,
θ_i is the voltage angle of bus i,
θ_j is the voltage angle of bus j,
n_l is the total number of branches in the network,
F_{loss} is the target/objective function to be minimized.

The objective function in (1) is intended to be minimized under the optimal siting and sizing of DGs subject to the following constraints:

Equality constraints: power flow equations satisfaction.
Inequality constraints:

The following expressions formulate the nodal voltage and branch currents constraints:

$$V_i^{\min} < V_i < V_i^{\max} \quad (2)$$

$$S_{branch\ j} < S_{branch\ j}^{\max} \quad (3)$$

where

$V_i^{\min}$ and $V_i^{\max}$ the lower and upper voltage limit of each bus, and $S_{branchj}^{\max}$ the ampacity level of each branch by terms of apparent power.

In this work two additional constraints are introduced in order to formulate the reverse power constraint and eventually to control it. It has to be mentioned that the problem of reverse power flow, when searching for the optimal penetration or installation of DG units in DNs towards loss minimization, has not been thoroughly examined and taken into account so far, based on the best knowledge of the authors. For example, in [6] it is mentioned that high embedded generation will export power through the feeder to the grid and may cause increase in losses along the way. [7] refers to evidence showing that the flow of power can be turned especially during high generation-low demand circumstances. In [8], it is argued that the impact of voltage rise, resulting from reverse power flow, would have implications on DG penetration to the grid. [9] refer to the problem by only explaining that for high penetration levels of DGs the network could experience bidirectional power flow. In [10] the authors provide only a simple constraint to refer to the existence of reverse power flow to the main busbar. In [11] an index is introduced and implemented to refer to the appearance of reverse power flow, during high generation-low demand instances. The reverse power flow constraint is formulated in this work under the following expressions:

$$-P_{Slackbus}^{Reverse} < \Delta P_{Slackbus}^{Optimum} \quad (4)$$

$$\left|\Delta P_{Slackbus}^{Optimum}\right| < \left|\Delta P_{Slackbus}^{Initial}\right| \quad (5)$$

where

$-P_{Slackbus}^{Reverse}$ is the permissible magnitude of reverse power flow,
$\Delta P_{Slackbus}^{Optimum} = P_{g,Slackbus}^{Optimum} - P_{d,Slackbus}^{Optimum}$ is the difference between the injected (produced – $P_{g,Slackbus}^{Optimum}$) and consumed (demanded – $P_{d,Slackbus}^{Optimum}$) active power at the slack bus for the final optimum solution after the siting and sizing of the DGs,
$\Delta P_{Slackbus}^{Initial}$ is the difference between the injected (produced – $P_{g,Slackbus}^{Initial}$) and consumed (demanded – $P_{d,Slackbus}^{Initial}$) active power at the slack bus before the DGs penetration.

The constraints in (4) and (5) have the following meaning:

- The optimal solution should not result in negative power difference at the slack bus; this indicates reverse power flow.
- The optimal solution should result in lower power difference at the slack bus than in the initial state with downstream power flow and no DG units; this indicates loss reduction in the network.

Under real operating conditions the constraints described in (4) and (5) describe the magnitude of the reverse power flow at the slack bus in terms of net active power. Thus, in order to define the optimal solution in these cases power dispatch is required. However this is not the case in this paper since the present analysis considers the reverse power flow constraint during the planning stage by the aggregator towards the best planning strategy for DG penetration towards loss minimization.

Thus, based on (4) and (5) the algorithm embeds flexibility concerning the permissible amount of reverse power flow. Therefore, limitations about the upper and lower amount of reverse flow could establish an additional constraint perspective, or alternatively the impact of various levels of reverse power flow to the optimal solution could be examined. In this analysis, the upper and lower levels of reverse power flow are set to the ampacity level of the main feeder at the slack bus, and to zero reverse power flow, respectively.

The problem is solved by a PSO algorithm and the objective function is minimized under the aforementioned constraints. These constraints are converted in penalty terms, as proposed in [22,23], and thus they are embedded in the updated objective function by the formulations that follow:

$$P(x) = f(x) + \Omega(x) \tag{6}$$

$$\Omega(x) = \rho\{g^2(x) + \max[(0, h(x))]^2\} \tag{7}$$

where

$P(x)$ is the penalty function,
$f(x)$ is the objective function (F_{loss}),
$\Omega(x)$ is the penalty term,
ρ is the penalty factor,
$g(x)$ is the equality constraints,
$h(x)$ is the inequality constraints.

Therefore, for the problem faced in this work the updated Penalty Function (PF) could be written as follows:

$$\mathrm{PF} = \min\left[F_{loss} + \rho(\Omega_P + \Omega_Q + \Omega_V + \Omega_L + \Omega_{\mathrm{Rev},1} + \Omega_{\mathrm{Rev},2})\right] \tag{8}$$

where

$$\Omega_P = \sum_{i=1}^{n_b}\left[g_{P,i}(V, \theta, P_g)\right]^2 \tag{9}$$

$$\Omega_Q = \sum_{i=1}^{n_b}\left[g_{Q,i}(V, \theta, Q_g)\right]^2 \tag{10}$$

$$\Omega_V = \sum_{i=1}^{n_b}\left[\max\left(0, V_i - V_i^{\max}\right)\right]^2 + \sum_{i=1}^{n_b}\left[\max\left(0, V_i^{\min} - V_i\right)\right]^2 \tag{11}$$

$$\Omega_L = \sum_{j=1}^{n_l}\left[\max\left(0, S_{linej} - S_{linej}^{\max}\right)\right]^2 \tag{12}$$

$$\Omega_{\mathrm{Rev},1} = \left[\max\left(0, -P_{SlackBus}^{\mathrm{Reverse}} - \Delta P_{SlackBus}^{Optimum}\right)\right]^2 \tag{13}$$

$$\Omega_{\mathrm{Rev},2} = \left[\max\left(0, \left|\Delta P_{SlackBus}^{Optimum}\right| - \left|\Delta P_{SlackBus}^{Initial}\right|\right)\right]^2 \tag{14}$$

PSO algorithm

Loss minimization is a non-linear optimization problem subject to several constraints and the dimensions of the problem could highly increase when solving the problem subject to optimal siting and sizing of DG units. The conventional approaches utilizing analytical methods could be complex and time consuming in this case [24]. Therefore, the problem is solved via a PSO algorithm which is considered to be an effective optimization strategy due to its ability to provide efficient solutions under minimum computational effort. PSO was initially introduced in 1995 by Kennedy and Eberhart [25], inspired by the social behavior of bird flocking or fish schooling. Several versions [26–29] have been developed since then in order to adjust the methodology to different optimization problems. In this work the version of the Local PSO (LPSO) variant [30] has been utilized; this PSO version is differentiated in regard to the Global PSO (GPSO) variant by terms of best particle definition. In GPSO variant, the personal best position of each particle found so far is compared with the global best position within the swarm. In LPSO variant, the global best is replaced by a local best defined within a smaller group of particles called neighborhood, thus it is actually the best position within a fictitious swarm which constitutes only a part of the whole initial swarm. The concept of LPSO is formulated as follows:

- If X_i is the ith particle of swarm $S = \{X_1, X_2, \ldots, X_N\}$ with $i = 1, \ldots, N$, then the neighborhood (NB) of X_i is defined as $NB_i = \{X_{n_1}, X_{n_2}, \ldots, X_{n_s}\}$, where $\{n_1, n_2, \ldots, n_s\} \subseteq \{1, 2, \ldots, N\}$ is the index set of its neighbors.
- $|NB_i|$ defines the size of the neighborhood.
- P_{g_i} indicates the best particle of neighborhood NB_i, thus $P_{g_i} = \arg\min_j f(P_j)$ with $j = n_1, n_2, \ldots, n_s \forall X_j \in NB_i$.

The structure of the neighborhoods is performed under the ring topology. More specific, each neighborhood is structured based on the particles' numbering as presented in the following expression:

$$NB_i = \{X_{i-r}, X_{i-r+1}, \ldots, X_{i-1}, X_i, X_{i+1}, \ldots, X_{i+r-1}, X_{i+r}\} \tag{15}$$

In (15), variable r defines the size of the neighborhood and is called neighborhood radius. The velocity and position of each particle are updated via the following expressions:

$$v_{ij}(t+1) = wv_{ij}(t) + c_1R_1(P_{ij}(t) - X_{ij}(t)) + c_2R_2(P_{gj}(t) - X_{ij}(t)) \tag{16}$$

$$X_{ij}(t+1) = X_{ij}(t) + v_{ij}(t+1) \tag{17}$$

where $i = 1, 2, \ldots, N$ and $j = 1, 2, \ldots, n$.

In (18) the inertia factor w is linearly decreased as follows:

$$w(t) = w_{up} - (w_{up} - w_{low})\frac{t}{T_{\max}} \tag{18}$$

where

t defines the iteration number of the algorithm implementation,
w_{up} is the upper limit of inertia,
w_{low} is the lower limit of the inertia,
$T_{\max}$ is the maximum number of iterations.

The selection of the LPSO algorithm is justified due to the fact that LPSO, in contrast with its global counterpart, provides more chances to avoid the local optima, due to its ability to provide a better balance between exploration and exploitation of the solution space. The complexity level of the LPSO algorithm depends on the problem's dimensions which in turn determine the length of each particle. Each particle consists of three parts: (a) the number of DGs (or nodes) to be installed, (b) the demand of each node regarding the generated active power, and (c) the demand of each node regarding the consumed or generated reactive power. In Fig. 1 the formulation of each particle is presented. Thus, given that the number of candidate DG units is n_g, the number of the dimensions results in $3n_g$. The optimum concerning the number of DG units to be installed is determined by the value of n_g, as follows:

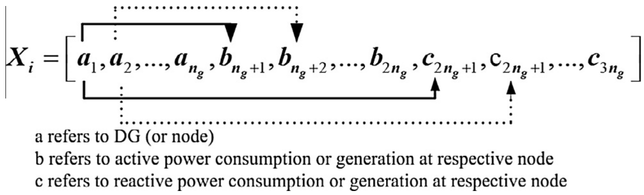

Fig. 1. Particle formulation based on dimensions' number.

- if $n_g < n_{total}$ (where n_{total} is the total number of the DN's nodes) then the algorithm seeks for optimal siting and sizing of a predefined number of DG units. This is defined here as *case study* optimal siting and sizing, and is the common approach of the vast majority of the published literature.
- if $n_g = n_{total}$ (proposed in this work) then the algorithm seeks for the optimal solution regarding (a) the number (since all nodes are candidate for DG installation), (b) the location, and (c) the type of the DG units, since for each node its needs about the consumed or generated active and reactive power are computed, to be installed altogether and simultaneously. The latter is considered crucial for the optimal solution since a sequential approach could be considered biased concerning the optimum of these three aforementioned dimensions of the problem.
- if $n_g > n_{total}$ approach is redundant since the algorithm will result in the same solution as above, but through an unnecessary strain.

As easily observed in Fig. 1, the particle is formed in such way that there is a correspondence for positions $k, n_g + k, 2n_g + k$ with $k = 1, \ldots, n_g$. In Table 1 the values of all variables included in the algorithm are summarized. All power flow analyses during the PSO implementation have been performed with the MATPOWER® [31] software package. It has to be mentioned that due to the heuristic nature of the PSO algorithm, the utilized version of PSO algorithm is this work has been applied 45 times for each solution. It was found that this number was adequate enough in order to come up with a better solution than the ones presented in literature.

DN under study and penetration scenarios

Examined DN

The proposed methodology about the optimal number, type, sizing and siting of DG units, has been applied to the IEEE 30 [32] bus system. This network has been selected due to the fact that five DG units are considered already installed in its initial state. This is actually the real case for many networks since the penetration level of RESs has been significantly increased during the last two decades. The basic problem regarding these large scale RESs penetration policies has been relied mainly on national and international energy policies related to environmental issues and have not been planned based on optimizing objectives like loss reduction. Therefore, for most existing networks the investigation of further DG or RESs penetration is expected to face the problem of potential reverse power flow due to already installed power units. That means, that in many cases the benefits of DG, e.g. loss reduction, would not be experienced, if appropriate consideration and planning is not taken into account. Moreover the proposed methodology has also been applied to the IEEE 33 [33] bus system in order to examine the impact of the reverse power flow constraint to the ODGP problem regarding a radial network with no installed DG units and under low load demand operating conditions. In Fig. 2 the layout of the 30 bus system is presented where it can be easily observed that nodes (labelled as PV nodes) 2, 13, 22, 23 and 27 have already DG units installed while the remaining (labelled as PQ nodes) are load nodes only. In Fig. 3 the 33 bus system is also illustrated. In Table 2, the basic data of the examined networks are presented.

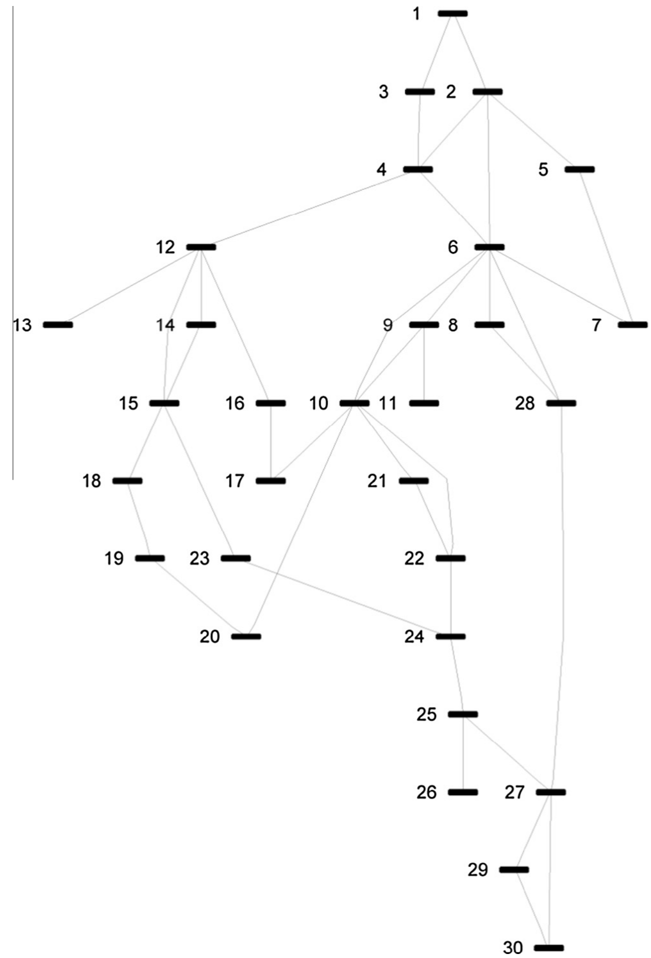

Fig. 2. IEEE 30 bus system.

Examined penetration scenarios

The impact of the permissible amount of reverse power flow to the optimal solution is examined through the following scenarios:

Table 1
Variable values for the proposed algorithm.

Variable	Value	Variable	Value
$c1$: coefficient of personal best	2.05	N: number of particles in swarm	30
$c2$: coefficient of global best (here neighborhood best)	2.05	r: neighborhood radius (neighborhood size)	2
w_{up}: inertia upper limit	0.9	T_{max}: maximum number of iterations	1000
w_{low}: inertia lower limit	0.4	Convergence tolerance	10^{-7}
p: penalty factor	10	Permissible level of reverse power flow	0 to unlimited

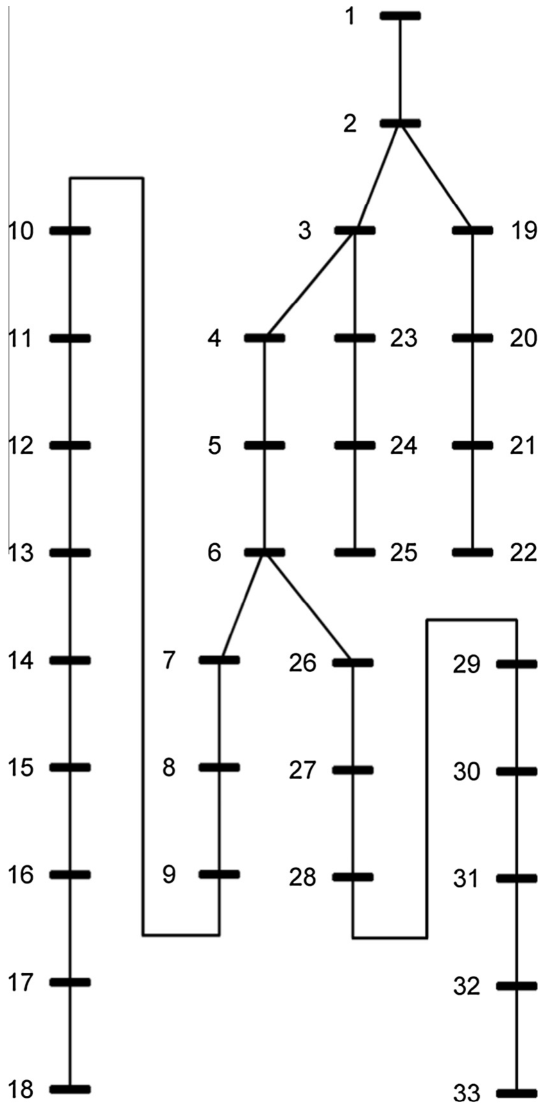

Fig. 3. IEEE 33 bus system.

the 1st one assumes that no reverse power flow is permitted, while the 2nd one considers no limitation (i.e. unlimited reverse power flow) about the reverse power flow. The optimal number of DG units to be installed is defined by setting $n_g = 30$ for 30 bus system and $n_g = 33$ for 33 bus system, which means that all nodes of the DN are candidates for DG installation. The other examined cases regarding the candidate nodes, i.e. 3, 5, and 10 units, constitute specific case studies concerning optimal allocation of a predefined number of DG units. Finally, the optimal sizing is defined by not setting boundaries about the active and reactive generation of the assumed DG unit. That means that the algorithm is expected to define the actual power needs of each node for loss minimization. Thus, there is no need for predefining the type of DGs to be installed since the resulted amount and kind (generated or demanded) power requirements could determine the type of one DG unit or a combination of different types of smaller units.

Results

The results provided by the proposed algorithm are presented in three subsections in order to highlight the respective contribution of the present work.

Impact of reverse power flow to the optimal solution

In Table 3, loss reduction about all penetration scenarios (implemented in IEEE 30 bus system,) is presented in regard to zero and unlimited permissible reverse power flow.

In Table 3 it can be easily observed that the optimal solution is affected by the permissible amount of reverse power flow when investigating the optimal penetration of DG units towards loss minimization. In most cases examined, especially for DNs with already installed DGs, the constraint of reverse power flow should be taken into account because the risk of estimating oversized capacity for the DG units could potentially cause additional problems related to congestion and overvoltage. Of course it should also be mentioned that loss reduction under no reverse power flow is lower in regard to the case that the constraint is not included in the solution process. Still, the worse solution in any case could be overweighed by the benefits of ensuring zero reverse power flow to the slack bus.

In Table 4 the results concerning the optimal solution of the ODGP problem (implemented in IEEE 33 bus system) for zero and unlimited permissible reverse power flow respectively, are presented. The results indicate that for this DN with no pre-installed DG units the optimal solution is not influenced regardless of the assumed scenario about the magnitude of the potential reverse power flow to the slack bus. This is because for the 33 bus system the total load demand is relatively low and there are no DG units already installed as well. Thus, the solution is not influenced by the permissible potential reverse power flow since the optimal solution refers to the optimal DG penetration for loss minimization and defines the maximum DG capacity towards this direction. This is due to the fact that based on the target function to be minimized (i.e. loss reduction) and the radial layout of the network the algorithm provides the same "optimal" solution no matter the setting for the permissible reverse power flow. Based on the nature of the bus 1 (i.e. slack bus) the algorithm finds out that reverse power flow

Table 2
Basic data of 30 bus system.

30 Bus system		33 Bus system	
Number of nodes 30	Number of branches 41	Number of nodes 33	Number of branches 32
Aggregated active power production (MW) 189.21	Aggregated reactive power production (MVAr) 0	Aggregated active power production (MW) 0	Aggregated reactive power production (MVAr) 0
Power base (MVA) 100	Voltage base (kV) 135	Power base (MVA) 100	Voltage base (kV) 12.66
Aggregated active power demand (MW) 189.2	Aggregated reactive power demand (MVAr) 107.2	Aggregated active power demand (MW) 3.72	Aggregated reactive power demand (MVAr) 2.3

Table 3
Impact of reverse power flow to optimal solution for 30 bus system.

Nodes (DGs) to be installed	No permissible reverse power flow Losses (MW)			Unlimited permissible reverse power flow Losses (MW)		
	Initial	Final	% Reduction	Initial	Final	% Reduction
3	2.44	1.154	**52.76**	2.44	1.057	**56.75**
5	2.44	0.995	**59.26**	2.44	0.854	**65.21**
10	2.44	0.918	**62.44**	2.44	0.755	**69.11**
30	2.44	0.918	**62.44**	2.44	0.727	**70.25**

could not exist for minimum power losses (even if the permissible reverse power flow is allowed to be unlimited the algorithm does not provide a solution that yields reverse power flow because for this latter case the losses would be increased and thus would not be minimum). Under low demand conditions the power flow across the network's branches is relatively small, thus since the algorithm tries to minimize power losses it is expected to provide a solution towards this direction with no reverse power flow. The latter means that the branch currents are expected to be decreased due to the installation of dispersed power units across the network as defined by the objective function. In most cases if the algorithm is somehow "forced" to cause reverse power flow, this could result in increased branch currents that would in turn cause power loss increase. In this work, the optimal solution binds the algorithm to conform to the goal concerning loss minimization. Under high load demand, the solution provided by the algorithm is more likely to cause reverse power flow since loss reduction could be achieved better under low upstream branch currents in respect to high downstream ones.

For this bus system, if already DG units had been existent then the penetration of additional DG capacity (even via the optimization process) could potentially cause reverse power flow.

Table 4
Impact of reverse power flow to optimal solution for 33 bus system.

Nodes (DGs) to be	Installation points (nodes to host DG unit)	No permissible reverse power flow Losses (MW)			Unlimited permissible reverse power flow Losses (MW)		
		Initial	Final	% Reduction	Initial	Final	% Reduction
3	3, 14, 30	0.211	0.0182	**91.37**	0.211	0.0182	**91.37**

Table 5
Optimal DG number.

DG number	Nodes identified	Optimal nodes number	Total active power injection (MW)	Total reactive power injection (MVAr)	% Loss reduction
No reverse power flow					
3	8, 19, 30	3	30.48	46.37	52.76
5	8, 17, 19, 24, 30	5	31.22	61.57	59.26
10	7, 8, 10, 12, 17, 19, 24, 26, 30	9	31.94	81.60	62.44
30	7, 8, 10, 12, 17, 19, 24, 26, 30	9	31.94	81.60	62.44
Optim. number		9			

Node 7	Node 8	Node 10	Node 12	Node 17	Node 19	Node 24	Node 26	Node 30
DG sizing for optimal solution with no reverse power flow								
0 MW	0 MW	6.802 MW	0 MW	8.516 MW	10.852 MW	0 MW	0 MW	5.465 MW
9.857 MVAr	28.65 MVAr	5.902 MVAr	9.978 MVAr	7.783 MVAr	5.304 MVAr	5.866 MVAr	2.456 MVAr	9.857 MVAr

DG number	Nodes identified	Optimal nodes number	Total active power injection (MW)	Total reactive power injection (MVAr)	% Loss reduction
Unlimited reverse power flow					
3	8, 10, 30	3	49.34	54.20	56.75
5	7, 8, 10, 19, 30	5	53.10	59.59	65.20
10	7, 8, 10, 17, 19, 24, 26, 30	8	53.94	69.68	69.11
30	6, 7, 8, 9, 10, 12, 14, 15, 16, 17, 18, 19, 21, 24, 26, 29, 30	17	52.77	87.81	70.25
Optim. number		17			

Node 7	Node 8	Node 10	Node 17	Node 19	Node 24	Node 26	Node 30
DG sizing for optimal solution with unlimited permissible reverse power flow							
9.548 MW	0 MW	15.93 MW	7.808 MW	12.438 MW	0 MW	1.326 MW	6.889 MW
9.438 MVAr	30.43 MVAr	3.749 MVAr	8.739 MVAr	5.337 MVAr	7.281 MVAr	2.343 MVAr	2.937 MVAr

Table 6
DG type installation for optimal solution with 10 nodes candidate for DG installation – no reverse power flow.

Optimal node position	Active power requirements (MW) (+ production, − consumption)	Reactive power requirements (MVAr) (+ production, − consumption)	Available DG types
No reverse power flow			
7	0	9.857	B
8	0	28.6554	B
10	6.8021	5.902	A, B, C
12	0	9.9788	B
17	8.5165	7.7825	A, B, C
19	10.8515	5.3043	A, B, C
24	0	5.8665	B
26	0	2.4564	B
30	5.465	2.9367	A, B, C

Table 7
Upstream power flow for DG penetration of 10 and 30 DG units.

DG penetration scenario – DG number	Optimal DG number	No reverse power flow Active power in slack bus (MW) (+ downstream, − upstream)	Unlimited reverse power flow Active power in slack bus (MW) (+ downstream, − upstream)
0 – initial state		0.25974	0.25974
3	3	−0.05775	−0.24757
5	5	−0.06696	−0.28722
10	9	−0.07493	−0.29651
30	17	−0.07187	−0.2851

Optimal number of DGs and optimal siting

The optimal number of DGs is performed by searching the highest possible distribution of power units for loss minimization. Therefore, the number of DG units is considered by the algorithm as the equal number of nodes to host DG units. Thus, instead of allocating a predefined number of power units with specified capacity the optimal number and position of the crucial nodes is provided by the present algorithm. The algorithm gradually increases the number of candidate nodes in order to find the optimal number. All results presented in this section refer to the IEEE 30 bust system. In Table 5 the results regarding the optimal number of nodes to install DG units is presented along with the aggregated requirements about the active and reactive power injection in the DN. For the case of no reverse power flow the optimal number is equal to 9, which results even if all nodes of the DN are considered candidate for DG installation. Moreover, the algorithm proves to converge about the aggregated requirements for active and reactive power production by the DG units. By that sense, the solution referring to 9 nodes to host DG with approximately 62.44% loss reduction under no reverse power flow is the optimal solution for this DN. For the case of unlimited reverse power flow the optimal solution refers to 17 installation points.

It should be clarified that the DG sizing for the optimal case under unlimited reverse power flow in Table 5, refers to 8 DG units and not 17 DG units as resulted. The reason for adopting as the optimal solution the one with 8 DG units relies on the following: this solution yields almost the same loss reduction as the one with 17 DG units under less than the half number of DG units which in turns keeps the dispersion level of the DG units in reasonable number.

Optimal sizing for DG type recommendation

In this section the sizing of DG units is correlated with the DG type by defining the active and reactive requirements for loss minimization of each node. Therefore, the type of DG is not predefined and the optimal solution is not restricted by type standardization. Thus, the type, or types, of DG units should be determined by the amount of active power generation requirements of each node, and of reactive power generation and/or consumption, respectively. The four commonly utilized DG types [12,14,16,17] are presented, but the algorithm's results regarding the minimum losses would define the combination of DG types to be installed. For example, in [12] although four types of DG are introduced, only one type is examined for each optimal solution. The same is performed in [14] and in addition siting and sizing of DG units are solved separately. In [16], only one DG type is examined at each time. Finally in [17], only two cases of DG types are essentially introduced and examined separately. In Table 6, the power requirements for each node obtained for the optimal solution, is presented. Based on these power needs, the algorithm proposes

Table 8
Comparison of proposed method with other existing approaches with active and reactive power generation – 30 bus system.

Method	Opt. DG number	Aggregated DG power (MW)–(MVAr)	% Loss reduction
Simplified method [34]	1	35–0	**30.68**
Complete analytical [35]	1	15–0	**6.82**
GA with fuzzy controller [36]	2	75–0	**22.74**
GA [37]	1	15–0	**6.82**
Proposed approach (no reverse power flow) – #1	9	31.63–78.74	**62.44**
Proposed approach (unlimited reverse power flow) – #2	17	52.77–87.81	**70.25**

Table 9
Comparison of proposed method with other existing approaches with active power generation – 30 bus system.

Method	Opt. DG number	Aggregated DG power (only MW)	% Loss reduction
Simplified method [34]	1	35	**30.68**
Complete analytical [35]	1	15	**6.82**
GA with fuzzy controller [36]	2	75	**22.74**
GA [37]	1	15	**6.82**
Proposed approach (no reverse power flow) – #3	9	32.65	**43.54**
Proposed approach (unlimited reverse power flow) – #4	17	54.50	**50.37**

the available mix of DG types to be installed in order to fulfil them. A respective table, like Table 6, has also resulted for the case of unlimited reverse power flow, in which it appears that one node should host DG type D. The available DG types are:

- Type A: DG with only active power production (e.g. PV, micro turbines, fuel cells).
- Type B: DG with only reactive power production (e.g. capacitors, synchronous compensators).
- Type C: DG with both active and reactive power production (e.g. synchronous generators).
- Type D: DG with active power production and reactive power consumption (e.g. induction generators).
- Type E: reactive power consumption (e.g. inductors, synchronous compensators).

The results in Table 7 indicate that for both penetration scenarios under unlimited reverse power flow, the upstream power flow to the slack bus is slightly higher than the respective downstream one at the initial case. Thus, both solutions could be considered feasible by terms of ampacity violations for the feeders starting from the slack bus.

Efficiency of the proposed methodology

In order to illustrate the effectiveness of the proposed methodology in this paper, the obtained results for the examined IEEE 30 bus system are compared with other four approaches from published literature that deal with the same DN towards optimal siting and sizing of DGs for loss minimization. In [34] a simplified analytical method compared to other analytical approaches is presented in order to speed up the process. In this work only one DG unit is examined to be installed and only one DG type is utilized, the one that considers only active power production. In [35] a complete analytical method is applied on 30 bus system for the optimal placement of DGs. As in [34] only one DG unit with only active power production is considered to be installed. The authors in [36] propose a methodology that combines a Genetic Algorithm (GA) with a fuzzy controller. The maximum number of DG units

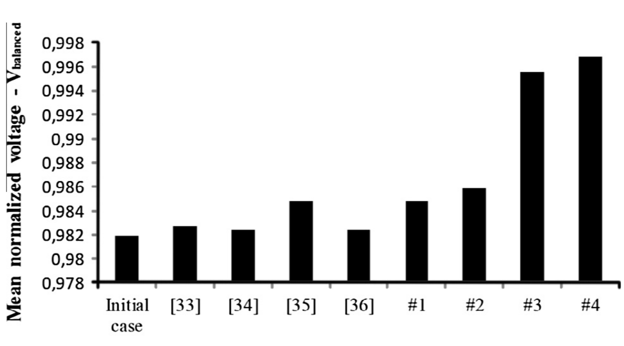

Fig. 4. Voltage profile for examined methods by terms of $V_{balanced}$ metric.

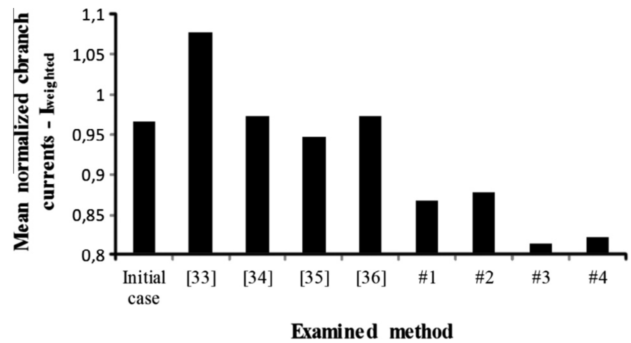

Fig. 5. Branch currents for examined methods by terms of $I_{weighted}$ metric.

to be installed is two, and again only active power production is assumed for them. Finally, in [37] a different GA is proposed but as in most papers only one DG unit with only active power production is examined to be optimally installed. Table 8 summarizes the results obtained by the approaches in [34–37] in comparison to the respective ones provided by the proposed algorithm in this work. The approaches #1–#4 that are included in Tables 8 and 9 refer to the following:

- #1 refers to the proposed solution in this work with both active power generation and reactive power generation/consumption of DG units under no reverse power flow,
- #2 refers to the proposed solution in this work with both active power generation and reactive power generation/consumption of DG units under unlimited permissible power flow,
- #3 refers to the proposed solution in this work with only active power generation of DG units under no reverse power flow,
- #4 refers to the proposed solution in this work with only active power generation of DG units under unlimited permissible reverse power flow.

In Table 8 the optimal solution of the proposed algorithm refers to both active and reactive power generation by the respective DG units while for all algorithms in [34–37] only active power generation is considered. Hence, the proposed algorithm has been applied again but for the case of only active power generation. The results, which now offer a direct comparison with methodologies in [34–37] are presented in Table 9. It is obvious in Table 9 that the proposed algorithm enhances the dispersed nature of the optimal penetration of DGs and as a result it yields better loss reduction in respect to the other four approaches. Moreover, the loss reduction is increased for the case of unlimited reverse power flow to the slack bus. Still, if no reverse power flow is allowed, loss reduction is approximately 42% higher by the best solution among the four approaches, i.e. solution in [34] 30.68%.

In order to quantify how balanced is the voltage profile of the DN in each case and how weighted are the carrying currents at all branches the following expressions are utilized:

$$V_{balanced} = \frac{\sum_{a=1}^{k} \frac{V_a}{V_{\text{nominal}}}}{k} \quad (19)$$

where
$V_{balanced}$ is the mean normalized voltage of the DN,
V_a is the voltage of node a,
V_{nominal} is the nominal voltage of the DN,
k is the total nodes number of the DN,

$$I_{weighted} = \frac{\sum_{b=1}^{n_l} \frac{I_b}{I_{b(ampacity)}}}{n_l} \quad (20)$$

where
$I_{weighted}$ is the total weighted current of the DN is respect to its ampacity level,
I_b is the current (rms) of branch b,
$I_{b(ampacity)}$ is the ampacity level (thermal limit of branch in terms of rms current) of branch b,
n_l is the total branch number of the DN.

The expression in (19) provides the mean normalized (pu. values) value of the nodes' voltage, while in (20) the current of each branch is normalized to its ampacity level which varies for the network's branches [32]. Therefore it is rational to accept that the metric in (19) describes how balanced is the voltage profile of the DN, while the one in (20) expresses how weighted are the carrying currents of the network. In Figs. 4 and 5, the values resulted by (19) and (20) for the methods presented in Tables 8 and 9 are respectively illustrated.

From Fig. 4 it is obvious that the proposed method in this work provides the most balanced voltage profile for the network. In fact, if both active and reactive power injections are considered for the assumed DG units, the voltage profile is improved in respect to the case where the DG units are considered to inject only active power. Moreover, the most important conclusion is that even under unlimited permissible reverse power flow, the metric $V_{balanced}$ does not exceed the nominal voltage of the network. In Fig. 5 the results indicate that the proposed approach yields significant current decrease in several branches after the DG installation. This is due to the fact that the proposed algorithm enhances the dispersion level of the required DG units for loss minimization, thus some branches experience carrying current decrease. The opposite is mostly seen in method [33] where it becomes obvious that the value of $I_{weighted}$ metric higher than one means that at least one (or more) branches undergo overloading with carrying currents higher than the considered ampacity level.

Conclusion

In this paper the optimization regarding the siting and sizing of DG units in DNs towards loss minimization is faced through a different and innovative perspective. So far, the common tactics relied on optimal allocation of predefined number of DG units with specified range about their capacity. Another widespread approach refers to analytical approaches concerning exhaustive investigation about the optimal location and capacity of limited DG units to be installed. In this work, minimum losses are computed by defining the optimal number of nodes along with their optimal power requirements which in turn expresses the optimal number and capacity of DG units to be installed. Moreover, the problem of loss minimization takes into account limitations about the permissible amount of reverse power flow to the slack bus of the network; these limitations are formulated by the form of a penalty term in the objective function. The proposed methodology consists of a LPSO variant algorithm with special considerations regarding the particles formulation and is applied on the widely utilized IEEE 30 and 33 bus systems. The results indicate that the proposed methodology is capable of resulting the optimal number, locations and capacity of DG units to be installed for loss minimization altogether. The impact of different permissible reverse power flow levels to the optimal solution is also illustrated and as proved it stands for networks with already DG units installed and high load demand. On the contrary, for DNs with no pre-installed DG units and low load demand the optimal solution is not affected by the potential permissible reverse power flow since the algorithm ensures that the optimal solution refers to the maximum capacity DG penetration for loss minimization without reverse power flow. Comparisons with other existing methodologies verify the superiority of the proposed technique by terms of higher loss reduction, since the optimization technique is not subject to any predefined input variables. That means, the algorithm is free to search for the optimal solution regarding all involved aspects referring to DG penetration, and yield the best solution about the distribution level of the units, their optimal behavior about power generation or consumption and their optimal location to be installed. It should be clarified that the proposed methodology provides the optimal solution regarding a specific snapshot of the network's operational conditions, i.e. the load composition of the network is assumed constant. Still, since the algorithm specifies the optimal locations and power requirements of the crucial nodes for DG installation, it could establish the appropriate context towards the optimal siting and sizing of DG units for energy minimization. In this latter case, the variability of the loads should be incorporated into the problem and the authors are currently investigating these potentials.

References

[1] Georgilakis PS, Member S, Hatziargyriou ND. Power distribution networks: models, methods, and future research. IEEE Trans Power Syst 2013;28:3420–8. http://dx.doi.org/10.1109/TPWRS.2012.2237043.

[2] Gözel T, Hocaoglu MH. An analytical method for the sizing and siting of distributed generators in radial systems. Electr Power Syst Res 2009;79:912–8. http://dx.doi.org/10.1016/j.epsr.2008.12.007.

[3] Abou El-Ela AA, Allam SM, Shatla MM. Maximal optimal benefits of distributed generation using genetic algorithms. Electr Power Syst Res 2010;80:869–77. http://dx.doi.org/10.1016/j.epsr.2009.12.02.

[4] Mohandas N, Balamurugan R, Lakshminarasimman L. Optimal location and sizing of real power DG units to improve the voltage stability in the distribution system using ABC algorithm united with chaos. Int J Electr Power Energy Syst 2015;66:41–52. http://dx.doi.org/10.1016/j.ijepes.2014.10.033.

[5] Ackermann T, Knyazkin V. Interaction between distributed generation and the distribution network: operation aspects. In: Transm distrib conf exhib 2002 Asia Pacific IEEE/PES, vol. 2; 2002. p. 1357–62. http://dx.doi.org/10.1109/TDC.2002.1177677.

[6] Masters CL. Voltage rise: the big issue when connecting embedded generation to long 11 kV overhead lines. Power Eng J 2002;16:5–12. http://dx.doi.org/10.1049/pe:20020101.

[7] Liew SN, Strbac G. Maximising penetration of wind generation in existing distribution networks. IEE Proc – Gener Transm Distrib 2002;149:256–62. http://dx.doi.org/10.1049/ip-gtd:20020218.

[8] Schwaegerl C, Bollen M. Voltage control in distribution systems as a limitation of the hosting capacity for distributed energy resources. In: 18th Int conf electr distrib. Turin: IET; 2005. p. 1–5.

[9] Méndez Quezada VH, Rivier Abbad J, Gómez San Román T. Assessment of energy distribution losses for increasing penetration of distributed generation. IEEE Trans Power Syst 2006;21:533–40. http://dx.doi.org/10.1109/TPWRS.2006.873115.

[10] Kalankul a., Jirapong P, Saraisuwan P, Premrudeepreechacharn S. Development of distributed generation assessment tool considering multi-system constraints for evaluating initial grid connection. In: Proc 2011 int conf util exhib power energy syst issues prospect Asia, ICUE 2011; 2012. p. 1–7. http://dx.doi.org/10.1109/ICUEPES.2011.6497751.

[11] Delfanti M, Falabretti D, Merlo M. Dispersed generation impact on distribution network losses. Electr Power Syst Res 2013;97:10–8. http://dx.doi.org/10.1016/j.epsr.2012.11.018.

[12] Hung DQ, Mithulananthan N, Bansal RC. Analytical expressions for DG allocation in primary distribution networks. IEEE Trans Energy Convers 2010;25:814–20. http://dx.doi.org/10.1109/TEC.2010.2044414.

[13] Abu-Mouti FS, El-Hawary ME. Heuristic curve-fitted technique for distributed generation optimisation in radial distribution feeder systems. IET Gener Transm Distrib 2011;5:172–80. http://dx.doi.org/10.1049/iet-gtd.2009.0739.

[14] Hung DQ, Mithulananthan N. Multiple distributed generator placement in primary distribution networks for loss reduction. IEEE Trans Ind Electron 2013;60:1700–8. http://dx.doi.org/10.1109/TIE.2011.2112316.
[15] Abu-Mouti FS, El-Hawary ME. Optimal distributed generation allocation and sizing in distribution systems via artificial bee colony algorithm. Power Deliv IEEE Trans 2011;26:2090–101. http://dx.doi.org/10.1109/TPWRD.2011.2158246.
[16] Moradi MH, Reza Tousi SM, Abedini M. Multi-objective PFDE algorithm for solving the optimal siting and sizing problem of multiple DG sources. Int J Electr Power Energy Syst 2014;56:117–26. http://dx.doi.org/10.1016/j.ijepes.2013.11.014.
[17] Murty VVSN, Kumar A. Optimal placement of DG in radial distribution systems based on new voltage stability index under load growth. Int J Electr Power Energy Syst 2015;69:246–56. http://dx.doi.org/10.1016/j.ijepes.2014.12.080.
[18] Moradi MH, Abedini M. A combination of genetic algorithm and particle swarm optimization for optimal DG location and sizing in distribution systems. Int J Electr Power Energy Syst 2012;34:66–74. http://dx.doi.org/10.1016/j.ijepes.2011.08.023.
[19] Gil Mena AJ, Martín García JA. An efficient approach for the siting and sizing problem of distributed generation. Int J Electr Power Energy Syst 2015;69:167–72. http://dx.doi.org/10.1016/j.ijepes.2015.01.011.
[20] Iyer H, Member S, Ray S, Ramakumar R, Fellow L. Assessment of distributed generation based on voltage profile improvement and line loss reduction. In: Transm distrib conf exhib; 2006. p. 1171–6.
[21] Viral R, Khatod DK. An analytical approach for sizing and siting of DGs in balanced radial distribution networks for loss minimization. Int J Electr Power Energy Syst 2015;67:191–201. http://dx.doi.org/10.1016/j.ijepes.2014.11.017.
[22] Leeton U, Uthitsunthorn D, Kwannetr U, Sinsuphun N, Kulworawanichpong T. Power loss minimization using optimal power flow based on particle swarm optimization. In: Electr eng comput telecommun inf technol (ECTI-CON), 2010 int conf; 2010. p. 440–4.
[23] Engelbrecht AP. Computational intelligence: an introduction. 2nd ed. John Wiley & Sons, Ltd.; 2007. http://dx.doi.org/10.1007/978-3-540-78293-3_1.
[24] Del Valle Y, Venayagamoorthy GK, Mohagheghi S, Hernandez J-C, Harley RG. Particle swarm optimization: basic concepts, variants and applications in power systems. IEEE Trans Evol Comput 2008;12:171–95. http://dx.doi.org/10.1109/TEVC.2007.896686.
[25] Eberhart R, Kennedy J. A new optimizer using particle swarm theory. MHS'95. In: Proc sixth int symp micro mach hum sci; 1995. p. 39–43. http://dx.doi.org/10.1109/MHS.1995.494215.
[26] Shi Y, Eberhart R. A modified particle swarm optimizer. In: 1998 IEEE int conf evol comput proceedings IEEE world congr comput intell (Cat No98TH8360); 1998. p. 69–73. http://dx.doi.org/10.1109/ICEC.1998.699146.
[27] Hu X, Shi Y, Eberhart R. Recent advances in particle swarm. In: IEEE congr evol comput 2004 CEC2004, vol. 1; 2004. p. 90–7. http://dx.doi.org/10.1109/CEC.2004.1330842.
[28] Mendes R, Kennedy J, Neves J. Watch thy neighbor or how the swarm can learn from its environment. In: Proc 2003 IEEE swarm intell symp SIS'03 (Cat. No. 03EX706); 2003. http://dx.doi.org/10.1109/SIS.2003.1202252.
[29] Kumar T, Thakur T. Comparative analysis of particle swarm optimization variants on distributed generation allocation for network loss minimization. In: First int conf networks soft comput; 2014. p. 167–71.
[30] Parsopoulos KE, Vrahatis MN. Particle swarm optimization and intelligence: advances and applications. Hershey: Information Science Reference; 2010. http://dx.doi.org/10.4018/978-1-61520-666-7.
[31] Zimmerman RD, Murillo-s CE. Matpower 4.1 user's manual. Power Syst Eng Res Cent 2011:1–116.
[32] Yokoyama R, Bae SH, Morita T, Sasaki H. Multiobjective optimal generation dispatch based on probability security criteria. IEEE Trans Power Syst 1987;3:317–24. http://dx.doi.org/10.1109/59.43217.
[33] Kashem MA, et al. A novel method for loss minimization in distribution networks. In: International conference on electric utility deregulation and restructuring and power technologies, 2000. Proceedings. DRPT 2000. IEEE; 2000. http://dx.doi.org/10.1109/DRPT.2000.855672.
[34] Ghosh S, Ghoshal SP, Ghosh S. Optimal sizing and placement of distributed generation in a network system. Int J Electr Power Energy Syst 2010;32:849–56. http://dx.doi.org/10.1016/j.ijepes.2010.01.029.
[35] Wang C, Member S, Nehrir MH, Member S. Analytical approaches for optimal placement of distributed generation sources in power systems April 17, 2006 Akarsh Sheilendranath. IEEE Trans Power Syst 2006;19:2068–76.
[36] Akorede MF, Hizam H, Aris I, Ab Kadir MZa. Effective method for optimal allocation of distributed generation units in meshed electric power systems. IET Gener Transm Distrib 2011;5:276–87. http://dx.doi.org/10.1049/iet-gtd.2010.019.
[37] Singh RK, Goswami SK. Optimum siting and sizing of distributed generations in radial and networked systems optimum siting and sizing of distributed generations in radial and networked systems. Electr Power Compon Syst 2009;37:127–45. http://dx.doi.org/10.1080/15325000802388633.